

The two-component system ArlRS is essential for wall teichoic acid glycoswitching in *Staphylococcus aureus*

Marieke M. Kuijk,¹ Emma Tusveld,¹ Esther Lehmann,² Rob van Dalen,¹ Iñigo Lasa,³ Hanne Ingmer,² Yvonne Pannekoek,¹ Nina M. van Sorge^{1,4}

AUTHOR AFFILIATIONS See affiliation list on p. 17.

ABSTRACT *Staphylococcus aureus* is among the leading causes of hospital-acquired infections. Critical to *S. aureus* biology and pathogenesis are the cell wall-anchored glycopolymers wall teichoic acids (WTA). Approximately one-third of *S. aureus* isolates decorates WTA with a mixture of α 1,4- and β 1,4-*N*-acetylglucosamine (GlcNAc), which requires the dedicated glycosyltransferases TarM and TarS, respectively. Environmental conditions, such as high salt concentrations, affect the abundance and ratio of α 1,4- and β 1,4-GlcNAc WTA decorations, thereby impacting biological properties such as antibody binding and phage infection. To identify regulatory mechanisms underlying WTA glycoswitching, we screened 1,920 *S. aureus* mutants (Nebraska Transposon Mutant Library) by immunoblotting for differential expression of WTA-linked α 1,4- or β 1,4-GlcNAc using specific monoclonal antibody Fab fragments. Three two-component systems (TCS), GraRS, ArlRS, and AgrCA, were among the 230 potential hits. Using isogenic TCS mutants, we demonstrated that ArlRS is essential for WTA β 1,4-GlcNAc decoration. ArlRS repressed *tarM* expression through the transcriptional regulator MgrA. In bacteria lacking *arlRS*, the increased expression of *tarM* correlated with the absence of WTA β 1,4-GlcNAc, likely by outcompeting TarS enzymatic activity. ArlRS was responsive to Mg^{2+} , but not Na^+ , revealing its role in the previously reported salt-induced WTA glycoswitch from α 1,4-GlcNAc to β 1,4-GlcNAc. Importantly, ArlRS-mediated regulation of WTA glycosylation affected *S. aureus* interaction with the innate receptor langerin and lysis by β 1,4-GlcNAc-dependent phages. Since WTA represents a promising target for future immune-based treatments and vaccines, our findings provide important insight to align strategies targeting *S. aureus* WTA glycosylation patterns during infection.

IMPORTANCE *Staphylococcus aureus* is a common colonizer but can also cause severe infections in humans. The development of antibiotic resistance complicates the treatment of *S. aureus* infections, increasing the need for antibiotic alternatives such as vaccines and therapies with bacterial viruses also known as phages. Wall teichoic acids (WTA) are abundant glycosylated structures of the *S. aureus* cell wall that have gained attention as a promising target for new treatments. Importantly, WTA glycosylation patterns show variation depending on environmental conditions, thereby impacting phage binding and interaction with host factors, such as antibodies and innate pattern-recognition receptors. Here, we show that the two-component system ArlRS is involved in the regulation of WTA glycosylation by responding to environmental changes in Mg^{2+} concentration. These findings may support the design of new treatment strategies that target WTA glycosylation patterns of *S. aureus* during infection.

KEYWORDS *Staphylococcus aureus*, wall teichoic acid, glycosylation, host-pathogen interactions, virulence regulation, two-component regulatory systems

Editor Victor J. Torres, St. Jude Children's Research Hospital, Memphis, Tennessee, USA

Address correspondence to Nina M. van Sorge, n.m.vansorge@amsterdamumc.nl.

The authors declare no conflict of interest.

See the funding table on p. 17.

Received 6 September 2024

Accepted 18 November 2024

Published 29 November 2024

Copyright © 2024 Kuijk et al. This is an open-access article distributed under the terms of the [Creative Commons Attribution 4.0 International license](https://creativecommons.org/licenses/by/4.0/).

Antimicrobial resistance is a global health crisis, which is estimated to cause an increasing number of deaths worldwide in the upcoming years (1). Infections caused by the Gram-positive pathogen *Staphylococcus aureus* are associated with high morbidity and mortality rates, and methicillin-resistant *S. aureus* specifically accounted for more than 100,000 deaths globally in 2019 (1). Consequently, *S. aureus* is one of six pathogens that significantly contributes to the number of multidrug-resistant deaths and is classified by the WHO as a high-priority pathogen (2). Novel treatments to combat these infections are therefore urgently needed.

Wall teichoic acids (WTA) are critical glycopolymers for *S. aureus* cell wall architecture, physiology, and host interaction. WTA molecules are covalently anchored to peptidoglycan and are composed of polyribitol-phosphate decorated with *N*-acetylglucosamine (GlcNAc) and D-alanine. WTA glycosylation plays an important role in a wide range of processes, including β -lactam resistance (3), phage infectivity (4, 5), and host interactions such as nasal colonization (6, 7), detection by WTA-specific antibodies (8–10), and the langerin receptor on skin Langerhans cells (11). The GlcNAc residues can be linked in several distinct orientations, resulting in structural heterogeneity of WTA. Nearly all *S. aureus* isolates glycosylate WTA with β 1,4-GlcNAc through the activity of the specific housekeeping glycosyltransferase TarS (3, 12). However, approximately one-third of *S. aureus* isolates can co-decorate WTA with α 1,4-GlcNAc through the activity of the glycosyltransferase TarM (12, 13). The *tarS* gene is part of the core genome and is co-localized with several other WTA biosynthesis genes, whereas *tarM* is located elsewhere in the genome (3, 14). Importantly, several of the WTA-mediated processes, for example, β -lactam resistance, langerin binding, and infection by specific phages, are dependent on WTA β 1,4-GlcNAc modification and may even be blocked by co-decoration with α 1,4-GlcNAc (15–17). The β 1,4-GlcNAc moiety is also a dominant target for human antibodies and is therefore an interesting target for immune-mediated treatments and vaccines (8, 10, 18). Clearly, these findings illustrate how changes in WTA glycosylation affect and shape host-pathogen interactions.

S. aureus can rapidly adapt its surface properties to different environmental conditions encountered during its commensal and pathogenic lifestyles, which is a major challenge for treating infections (19, 20). One of these adaptations relates to different glycosylation patterns of the cell wall that may favor bacterial survival in specific niches. Indeed, *S. aureus* can shift the abundance of α 1,4-GlcNAc and β 1,4-GlcNAc WTA glycosylation depending on the environmental conditions. For example, bacteria grown *in vitro* under rich growth conditions primarily decorate WTA with α 1,4-GlcNAc, whereas *S. aureus* isolated from organs after murine infection or after culture in high salt conditions express predominantly β 1,4-GlcNAc WTA (8, 21). Culture density also affects α 1,4-/ β 1,4-GlcNAc WTA glycosylation ratios through quorum sensing, as auto-inducing peptides have been observed to reduce *tarM* expression in stationary cultures, resulting in increased phage-mediated lysis (22). Although these examples illustrate the ability of *S. aureus* to switch between α 1,4- or β 1,4-GlcNAc-dominated WTA glycosylation profiles, the underlying molecular mechanisms and regulatory pathways are currently unknown.

Key to the virulence of *S. aureus* as a pathogen is its ability to quickly adapt its gene expression profile (23, 24) through a network of transcriptional regulators (SarA, Rot, MgrA, among others), alternative sigma factors (SigB and SigH) (23) and two-component systems (TCS) (25). *S. aureus* encodes 16 TCS, of which only WalRK is essential (25, 26). TCS recognize specific external triggers by a sensing histidine kinase, leading to transcriptional regulation through the phosphorylated response regulator (27). Intriguingly, no major growth defects were observed in a *S. aureus* mutant lacking all 15 non-essential TCS under standard laboratory conditions (25). However, many TCS, such as AgrCA, SaeRS, SrrAB, and ArlRS, have been shown to increase bacterial virulence or survival in certain *in vivo* conditions (23, 27). With regard to WTA glycosylation, only AgrCA has been experimentally implicated in the transcriptional regulation of *tarM* (22). Also, GraRS has also been implicated in the regulation of *tarM* (28), although this has not been functionally verified at the level of WTA glycosylation.

The TCS ArlRS has also been linked to WTA, but as a repressor of the *dlt* operon encoding the machinery for WTA D-alanylation (29). In addition, ArlRS is important in regulating host interaction processes such as adhesion and damage to endothelial cells (30, 31), clumping with fibrinogen (31–33), and expression of several immune evasion factors that block neutrophil killing (34). Although the exact triggers to activate ArlRS in *S. aureus* are not yet known, ArlRS has been implicated in the homeostasis of the essential divalent cations Mn^{2+} and Mg^{2+} (29, 35, 36).

The regulatory mechanisms that control WTA glycoswitching in response to varying environmental conditions remain largely unknown. This study aimed to identify key regulators and unravel the molecular mechanisms involved in the differential expression of α 1,4- and β 1,4-GlcNAc phenotypes. We demonstrated that ArlRS is essential for β 1,4-GlcNAc decoration of WTA, which impacted phage infection and langerin interaction. In addition, ArlRS was required for the Mg^{2+} -induced glycoswitch from α 1,4- to β 1,4-GlcNAc WTA glycosylation *via* the transcription factor MgrA. Given that WTA represents a promising target for future immune-based treatments and vaccines, our findings are of significance when designing new strategies that align with the WTA glycosylation patterns of *S. aureus* during infection.

RESULTS

Environmental conditions affect *tarM*, but not *tarS* transcription levels

S. aureus strains carrying both *tarM* and *tarS* can co-decorate WTA with α 1,4- and β 1,4-GlcNAc, respectively. To understand the molecular mechanisms underlying the modification of the α 1,4- and β 1,4-GlcNAc ratio in response to environmental conditions (21), we investigated how expression levels of *tarM* or *tarS* are affected in different environments. We therefore re-analyzed a previously published transcriptomics data set of *S. aureus* strain HG001 across 44 different conditions ranging from *in vitro* laboratory culture to *in vivo*-mimicking host environments (24). From this data set, we extracted transcription data for the *tarM* and *tarS* genes (37) and compared the variance of the expression levels of the two genes across these conditions. Expression of *tarM* fluctuated substantially, and this variance significantly differed from the more stable *tarS* expression in these 44 experimental conditions (Fig. 1). These results suggest that shifts in the WTA glycosylation profile are predominantly regulated through *tarM* rather than *tarS*.

Multiple two-component systems are identified to be involved in WTA glycoswitching

Given the dynamic regulation of *tarM*, we next aimed to identify the genes that may be involved in this process. To this end, we screened the Nebraska Transposon Mutant Library (NTML), containing 1,920 arrayed mutants, for differential α 1,4- and β 1,4-GlcNAc expression (38). Importantly, the NTML parental strain JE2 harbors both *tarM* and *tarS* genes. To facilitate high-throughput screening, we used immunoblotting of individual transposon mutants. A representative control immunoblot containing JE2 wild type (WT) and the markerless deletion mutants $\Delta tarMS$, $\Delta tarM$, and $\Delta tarS$ in the same background is visualized in Fig. 2A. We then performed two parallel screens using Fab fragments that specifically detect α 1,4- and β 1,4-GlcNAc WTA (Fig. 2B) (39).

We identified 230 genes potentially involved in WTA glycosylation (Table S1). Importantly, the transposon mutants *tarM* (SAUSA300_0939) and *tarS* (SAUSA300_0252) were identified as non-binding mutants in their respective 4461 and 4497 screens, thereby acting as positive controls of this unbiased screening method. Among the 230 potential genes, 115 were identified in the α 1,4-GlcNAc and 115 in the β 1,4-GlcNAc screen (Fig. 2C; Table S1). A higher number of transposon mutants exhibited upregulated WTA glycosylation compared to the number of mutants in which it was downregulated (195 compared to 35; Fig. 2C). Ten mutants showed high binding to both Fabs, whereas 14 genes had a differential effect on α 1,4- and β 1,4-GlcNAcylation (Fig. 2C). Of interest, we identified six genes of three different TCS (GraRS, ArlRS, and AgrCA) in the 4461

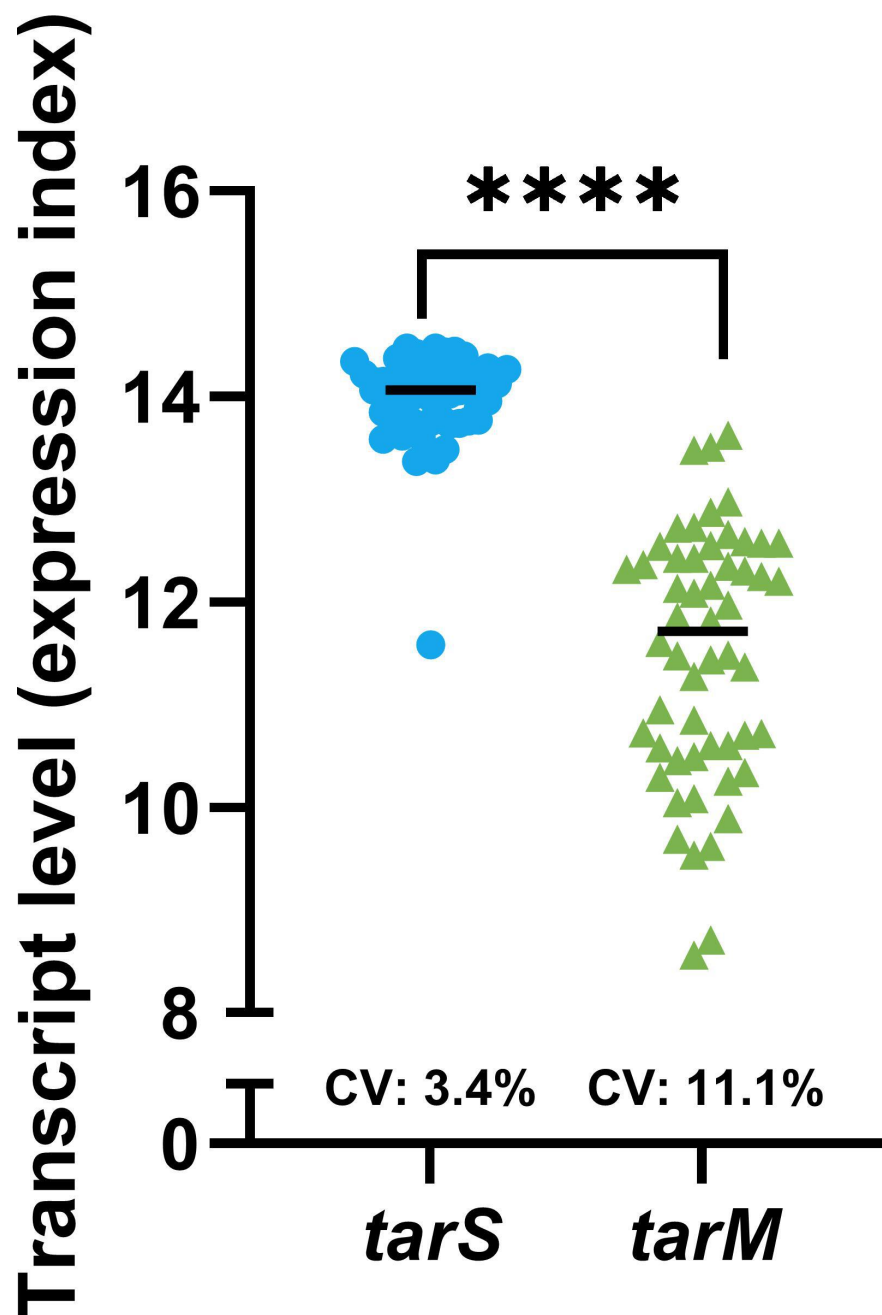


FIG 1 *tarM* expression is dynamically regulated. Transcript levels of *tarS* (SAOUHSC_00228) and *tarM* (SAOUHSC_00973) of *S. aureus* HG001 in 44 different *in vitro* and *in vivo*-mimicking conditions. The coefficient of variation (CV) of both data sets is shown. Data are extracted from Mäder *et al.* (24, 37). The variance of the two genes was statistically tested using an F test. **** $P < 0.0001$.

(α 1,4-GlcNAc) screen (Table 1). In addition, nine transcriptional regulators were identified across both screens (Table 1).

Two-component system ArlRS is essential for WTA β -GlcNAc expression

Based on the identification of three different TCS, we next aimed to confirm the role of these TCS in regulating WTA glycosylation. We first analyzed 4461 and 4497 Fab binding to a markerless deletion mutant lacking all 15 non-essential TCS (Δ XV) using flow cytometry (25), and observed that this mutant completely lacked WTA β 1,4-GlcNAc

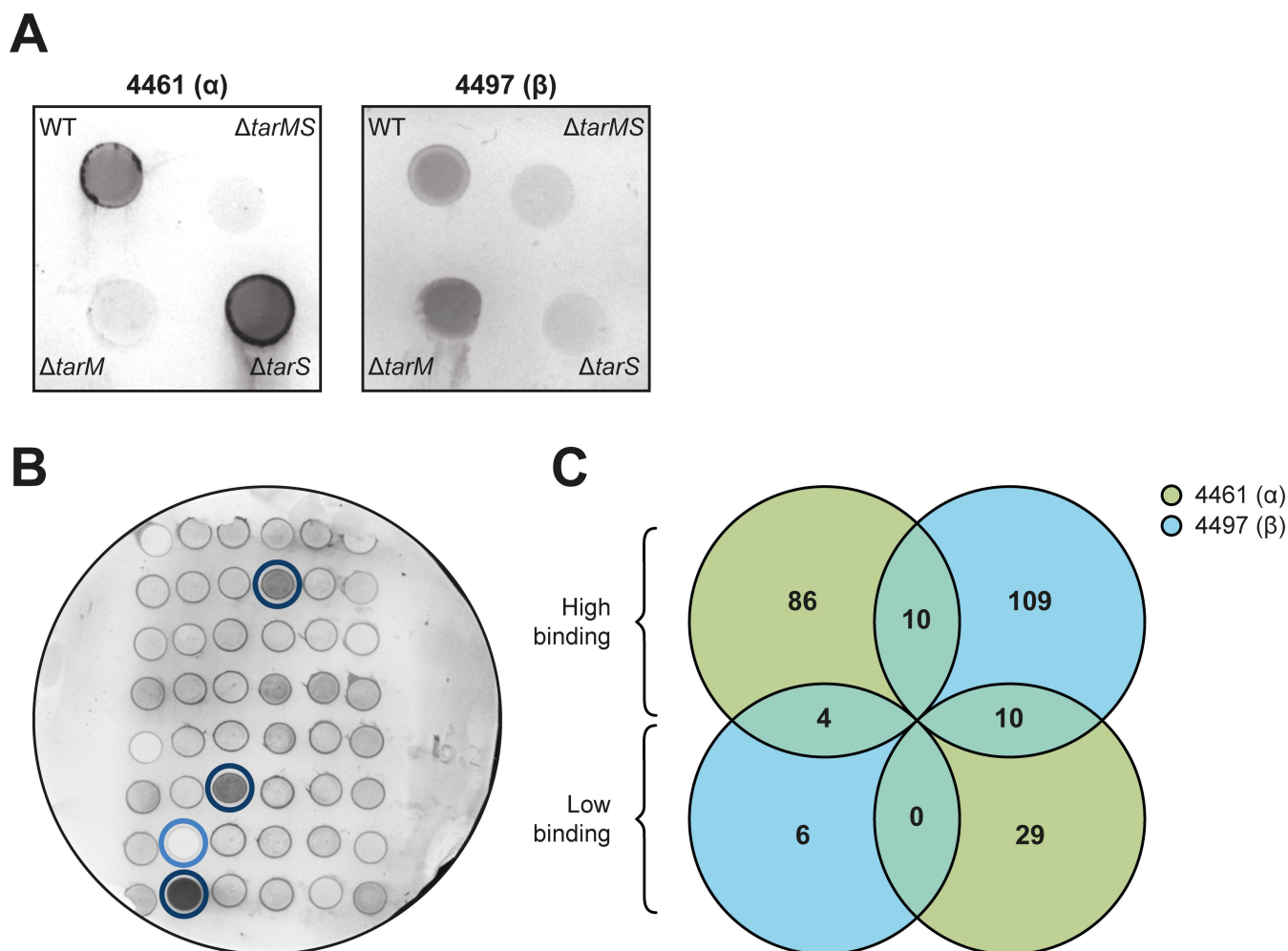


FIG 2 Representative immunoblot and Venn diagram summarizing results from the NTML screen to identify WTA glycoswitch mutants. (A) Representative immunoblot of JE2 WT and deletion mutants $\Delta tarMS$, $\Delta tarM$ and $\Delta tarS$ in JE2 background stained with 4461 or 4497 (B) Representative image of an immunoblot containing 48 NTML mutants screened for binding of 4461 (α 1,4-GlcNAc). Three transposon mutants show comparatively high binding (encircled in dark blue) and one transposon mutant shows low binding (encircled in light blue). (C) Venn diagram with a number of NTML mutants identified with either high or low levels of α 1,4- (in blue) and β 1,4-glycosylation (in green). The number of overlapping mutants is also depicted.

glycosylation (Fig. 3A). Further analysis of three isogenic TCS mutants, $\Delta arlRS$, $\Delta agrCA$, and $\Delta graRS$, showed that the WTA glycosylation phenotype of the $\Delta arlRS$ mutant was similar to the ΔXV mutant with regard to β 1,4-glycosylation, but additionally showed significantly increased α 1,4-GlcNAc levels (Fig. 3A). By contrast, deletion of $graRS$ and $agrCA$ did not significantly alter α 1,4- or β 1,4-GlcNAc WTA glycosylation levels (Fig. 3A). The β 1,4-GlcNAc-deficient phenotype of ΔXV and $\Delta arlRS$ was completely rescued through $arlRS$ plasmid complementation (Fig. 3B), demonstrating that $arlRS$ is essential for the expression of WTA β 1,4-GlcNAc expression in our assay conditions. As the growth phase of bacteria can affect glycosylation (22), we compared the growth characteristics of WT bacteria, $\Delta arlRS$ and $\Delta arlRS$ $parlRS$ mutants (Fig. S1A and C). No growth deficits were seen in either the growth curves or the CFU per mL overnight culture (Fig. S1). This indicates that the differences in WTA glycosylation are due to the $ArIRS$ TCS rather than culture density changes.

To investigate whether $ArIRS$ regulated the expression of $tarM$ or $tarS$, we quantified the absolute copy numbers of $tarM$ and $tarS$ by qPCR. The $\Delta arlRS$ mutant showed a substantial increase in $tarM$ copy number compared to WT, which was reversed by complementing the mutant with plasmid-expressed $arlRS$. By contrast, no changes were observed between the $tarS$ copy numbers of WT, $\Delta arlRS$, and the complemented mutant

TABLE 1 Identified transposon mutants in two-component systems and regulatory proteins^a

Accession No.	NTML ID	Gene	Description	Fab binding	
				4461 (α)	4497 (β)
Two-component systems					
SAUSA300_0646	NE1756	<i>graS</i>	Sensor protein kinase GraS	High	-
SAUSA300_1307	NE1183	<i>arlS</i>	Sensor histidine kinase protein	High	-
SAUSA300_1308	NE1684	<i>arlR</i>	DNA-binding response regulator	High	-
SAUSA300_1989	NE95	<i>agrB</i>	Accessory gene regulator protein B	High	-
SAUSA300_1991	NE873	<i>agrC</i>	Accessory gene regulator protein C	High	-
SAUSA300_1992	NE1532	<i>agrA</i>	Accessory gene regulator protein A	High	-
Regulators					
SAUSA300_0114	NE165	<i>sarS</i>	Staphylococcal accessory regulator	Low	High
SAUSA300_0605	NE1193	<i>sarA</i>	Accessory regulator A	High	-
SAUSA300_0647	NE645	<i>vraF</i>	ABC transporter, ATP-binding protein	High	-
SAUSA300_1708	NE386	<i>rot</i>	Staphylococcal accessory regulator Rot	Low	High
SAUSA300_2022	NE1109	<i>rpoF</i>	RNA polymerase sigma factor SigB	High	High
SAUSA300_2025	NE1607	<i>rsbU</i>	Sigma-B regulation protein	High	High
SAUSA300_2326	NE1304	-	Transcription regulatory protein	Low	-
Other					
SAUSA300_0023	NE1865	<i>yycI</i>	YycI protein (regulation WalRK)	High	-
SAUSA300_2075	NE149	<i>rho</i>	Transcription termination factor (regulation SaeRS)	-	High

^aGlycosylation patterns of NTML mutants were assessed with high, low or average (–) levels of Fab binding of 4461 (α1,4-GlcNAc) or 4497 (β1,4-GlcNAc).

(Fig. 3C). To assess whether increased *tarM* copy numbers correlated with increased promoter activity, we used an sGFP-reporter system in which the *tarM* promoter region was fused to *gfp* in plasmid pCM29 (40). This plasmid was transformed into WT and Δ *arlRS* to create WT pP_{*tarM*}-*gfp* and Δ *arlRS* pP_{*tarM*}-*gfp*. Δ *arlRS* showed a significantly increased *tarM* promoter activity compared to WT (Fig. 3D). These data indicate that *ArlRS* acts as a repressor of *tarM* expression, promoting WTA β1,4-GlcNAc decoration.

High Mg²⁺ concentrations drive WTA glycoswitching

High salt concentrations are known to induce a shift in *S. aureus* WTA glycosylation patterns from predominantly α1,4-GlcNAc to β1,4-GlcNAc decoration (21). The high salt medium previously used contained both Mg²⁺ (15 g/L MgCl₂ = 158 mM) and Na⁺ (41 g/L NaCl = 702 mM) to induce a stress response. Previously, *ArlRS* activity was linked to the presence of the divalent cation Mg²⁺ (29). To investigate whether the salt-induced WTA glycoswitch depended on Mg²⁺ or Na⁺, WT and Δ *arlRS* were grown in TSB and TSB supplemented with either 200 mM Mg²⁺ (TSB + Mg²⁺) or 200 mM Na⁺ (TSB + Na⁺). These salt concentrations did not alter bacterial growth (Fig. S1B and C). WTA glycosylation was assessed by binding of Fabs 4461 and 4497. Corresponding to previous findings, Mg²⁺ strongly affected WTA glycosylation levels in WT and complemented Δ *arlRS* *parlRS* bacteria, with a significant decrease of 4461 (α1,4-GlcNAc) Fab binding and concomitant increase in 4497 (β1,4-GlcNAc) Fab binding compared to growth in TSB (Fig. 4A). By contrast, the addition of Na⁺ only slightly increased levels of β1,4-GlcNAc, but had no significant effect on α1,4-GlcNAc levels (Fig. 4A). No differences in α1,4- and β1,4-GlcNAc levels were observed in Δ *arlRS* when grown in TSB supplemented with Mg²⁺ or Na⁺ compared to growth in TSB only. These results suggest that salt-induced glycoswitching is driven by Mg²⁺, but not Na⁺, and is *ArlRS*-dependent under the growth conditions used. We next assessed whether the Mg²⁺-induced WTA glycoswitch was caused by changes in *tarM* promoter activity using our sGFP transcriptional reporter system. Mg²⁺ strongly reduced *tarM* promoter activity in WT but not in the Δ *arlRS* mutant (Fig. 4B). These results suggest that Mg²⁺ signals through *ArlRS* to repress *tarM* promoter activity, which results in increased β1,4-GlcNAc levels.

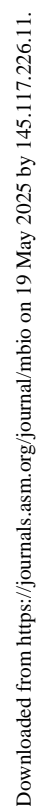
10.1128/mbio.02668-24 **7**

Fig 3 (Continued)

and *tarS* as measured with qPCR in WT, Δ *arlRS*, and complemented bacteria. Symbols below the dotted line represent extrapolated values. (D) sGFP fluorescence as a measure for promoter activity of *tarM* in WT $pP_{tarM-gfp}$ or Δ *arlRS* $pP_{tarM-gfp}$ bacteria as analyzed by flow cytometry and represented as fluorescence intensity (FI). Data are shown as three biological replicates \pm SEM. Statistical significance was determined using one-way ANOVA with Bonferroni statistical hypothesis testing to correct for multiple comparisons (A, B, C) and Student's t test (D). For panel (A), the mean of each column was compared to WT marking only significant comparisons. * $P < 0.05$, ** $P < 0.01$, *** $P < 0.001$, **** $P < 0.0001$, ns = not significant.

TCS ArlRS represses *tarM* expression through MgrA

In previous research, *tarM* was not identified as part of the ArlRS regulon (41). However, regulation could be indirect since ArlRS tightly regulates the expression of the global transcriptional regulators *mgrA* and *spx* by binding to a sequence motif in the promoter region. In turn, MgrA and Spx control the expression of numerous downstream genes (33, 41). To investigate the link between ArlRS and *tarM* regulation, we analyzed the activity of the *spx* and *mgrA* promoters with the sGFP-reporter system in both WT and

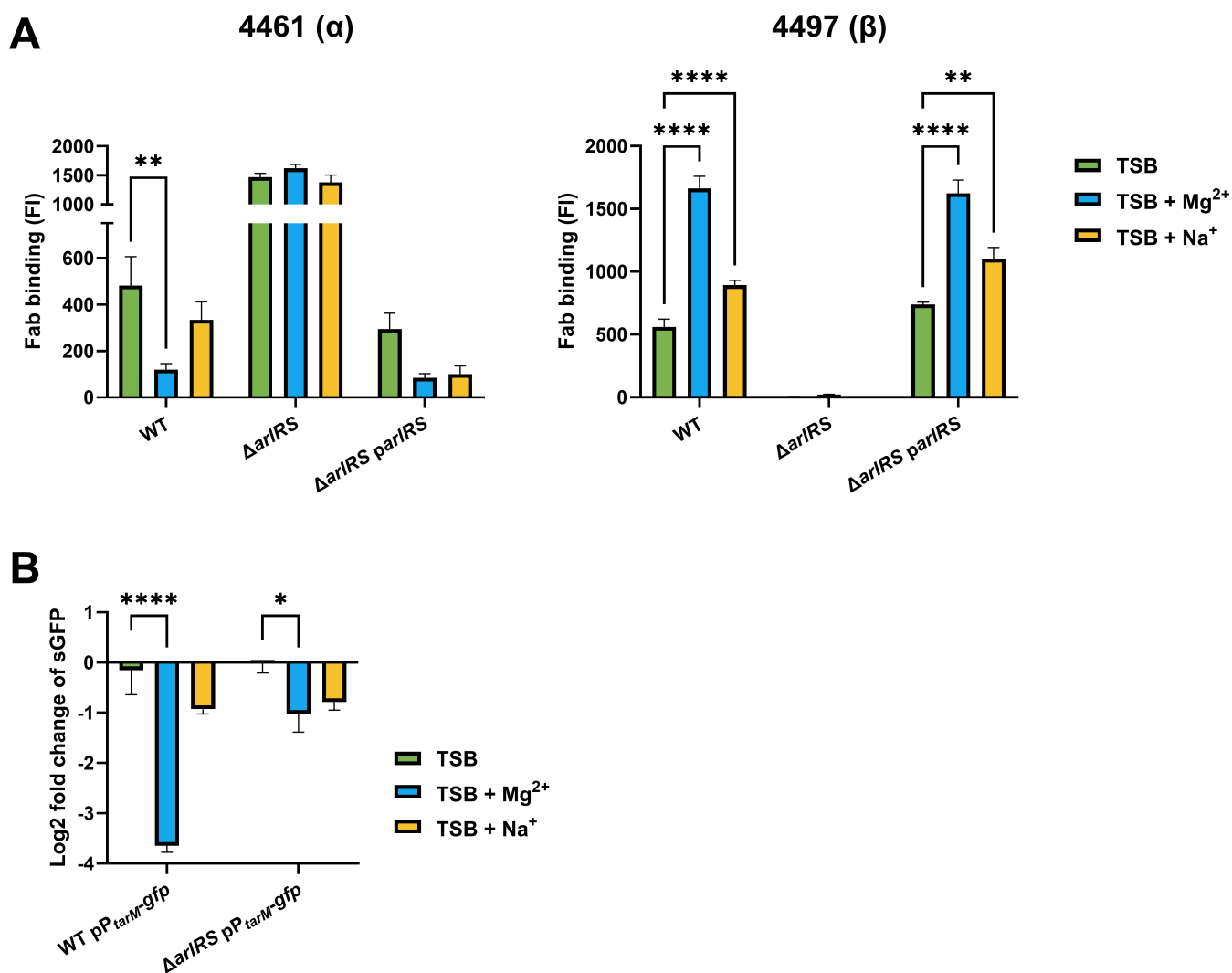


FIG 4 Mg^{2+} drives WTA glycoswitch towards β 1,4-GlcNAc and is ArlRS dependent. (A) Levels of WTA α 1,4- and β 1,4-GlcNAc, quantified by binding of Fab fragments 4461 (α) and 4497 (β) to WT, Δ *arlRS* and Δ *arlRS* *parlRS* when grown in TSB or TSB supplemented with 200 mM Mg^{2+} or 200 mM Na^+ . Data are represented as fluorescence intensity (FI) as analyzed by flow cytometry. (B) Promoter activity of *tarM*, displayed as log₂ fold change in fluorescence intensity of sGFP in WT $pP_{tarM-gfp}$ or Δ *arlRS* $pP_{tarM-gfp}$ bacteria grown in TSB supplemented with 200 mM Mg^{2+} or 200 mM Na^+ compared to regular TSB. Data represent three biological replicates \pm SEM. Statistical significance was determined using two-way ANOVA with Bonferroni statistical hypothesis testing to correct for multiple comparisons. The mean of each column was compared to the mean of TSB marking only significant comparisons. * $P < 0.05$, ** $P < 0.01$, *** $P < 0.001$, **** $P < 0.0001$.

the $\Delta arlRS$ mutant strain. sGFP fluorescence was measured after overnight culture in TSB containing 50, 100, or 200 mM of Mg^{2+} or Na^+ and was compared to fluorescence of bacteria grown in TSB only. We observed a dose-dependent increase in *mgrA* promoter activity in response to Mg^{2+} , but not Na^+ (Fig. 5A). By contrast, the *spx* promoter did not respond to the addition of Mg^{2+} or Na^+ in the medium (Fig. 5A). These observations suggest that Mg^{2+} drives the WTA glycoswitch through ArlRS-dependent activation of *mgrA*.

We postulated that MgrA is part of the regulatory network of ArlRS-dependent WTA glycosylation. To confirm this experimentally, the native *mgrA* promoter was exchanged with a cadmium-inducible promoter in the $\Delta arlRS$ mutant ($\Delta arlRS$ P_{Cd} -*mgrA*). Importantly, the $\Delta arlRS$ P_{Cd} -*mgrA* strain expressed *mgrA* and *tarM* mRNA at levels comparable to those in WT and $\Delta arlRS$ *parlRS* (Fig. S2). Chromosomal exchange of P_{Cd} -*mgrA* restored WTA α 1,4-GlcNAc and β 1,4-GlcNAc glycosylation to WT levels (Fig. 5B). Remarkably, while the $\Delta mgrA$ mutant showed the absence of β 1,4-GlcNAc, it maintained normal levels of α 1,4-GlcNAc compared to WT (Fig. 5B). These results indicate that MgrA is involved in the ArlRS-dependent WTA glycosylation.

To investigate whether the deletion of *mgrA* also influences *tarM* promoter activity, we transformed the pP_{tarM} -*gfp* plasmid in $\Delta mgrA$, creating $\Delta mgrA$ pP_{tarM} -*gfp* and compared its sGFP levels with WT and $\Delta arlRS$. Similar to $\Delta arlRS$, $\Delta mgrA$ showed a significantly increased *tarM* promoter activity compared to WT (Fig. 5C). Collectively, these results indicate that ArlRS regulates WTA glycoswitching through the transcription factor MgrA, which represses *tarM* transcription. The proposed pathway is visualized in Fig. 5D.

ArlRS affects β 1,4-GlcNAc-dependent functions as langerin binding and phage infection

To assess the functional consequences of ArlRS-dependent glycoswitching, we explored its effects on β 1,4-GlcNAc-mediated processes, including antibiotic susceptibility, langerin binding, and phage susceptibility.

We have previously shown that langerin, a C-type lectin receptor of Langerhans cells, recognizes *S. aureus* WTA β 1,4-GlcNAc, which subsequently initiates an inflammatory response in the skin (11). We hypothesized that ArlRS could affect langerin binding, thereby impacting the first response of Langerhans cells. Using recombinant FITC-labeled constructs of the extracellular domains of langerin, we observed that langerin binding was greatly diminished in bacteria lacking *arlRS* compared to WT bacteria (Fig. 6A). This phenotype could be restored by complementing *arlRS* (Fig. 6A). Correspondingly, langerin binding to WT bacteria could be further enhanced by supplementing the culture medium with Mg^{2+} , but not Na^+ (Fig. 6B). In line with our hypothesis, langerin binding to the $\Delta arlRS$ mutant was not affected by the addition of Na^+ or Mg^{2+} .

WTA glycosylation also affects phage infection as some phages, for example, Stab20 and Stab20-like phages such as vB_SauM_EW72 (22), require WTA β -GlcNAc moieties to bind to and subsequently infect *S. aureus* (16, 17). We therefore tested the phage susceptibility of our strains. As shown previously (22), we observed phage infection of WT bacteria, with clearly visible plaques that averaged 4×10^7 PFU/mL (Fig. 6C; Fig. S3). However, no plaques were observed in the $\Delta arlRS$ mutant, indicating a 7-log difference in infectivity (Fig. 6C). Supplementation with Mg^{2+} , but not Na^+ , enhanced infection by some phages in WT bacteria, although this effect was relatively minor (Fig. 6D; Fig. S4).

Finally, previous research showed that β 1,4-GlcNAc decoration contributes to β -lactams resistance in MRSA (3). We confirmed that the $\Delta arlRS$ mutant was more sensitive to oxacillin, but remained resistant to penicillin, compared to WT and $\Delta arlRS$ *parlRS* (Fig. S5). Together, langerin binding, phage infection data, and antibiotic susceptibility assays demonstrate that ArlRS-dependent glycoswitching has biologically relevant consequences in host and phage interaction and antibiotic resistance.

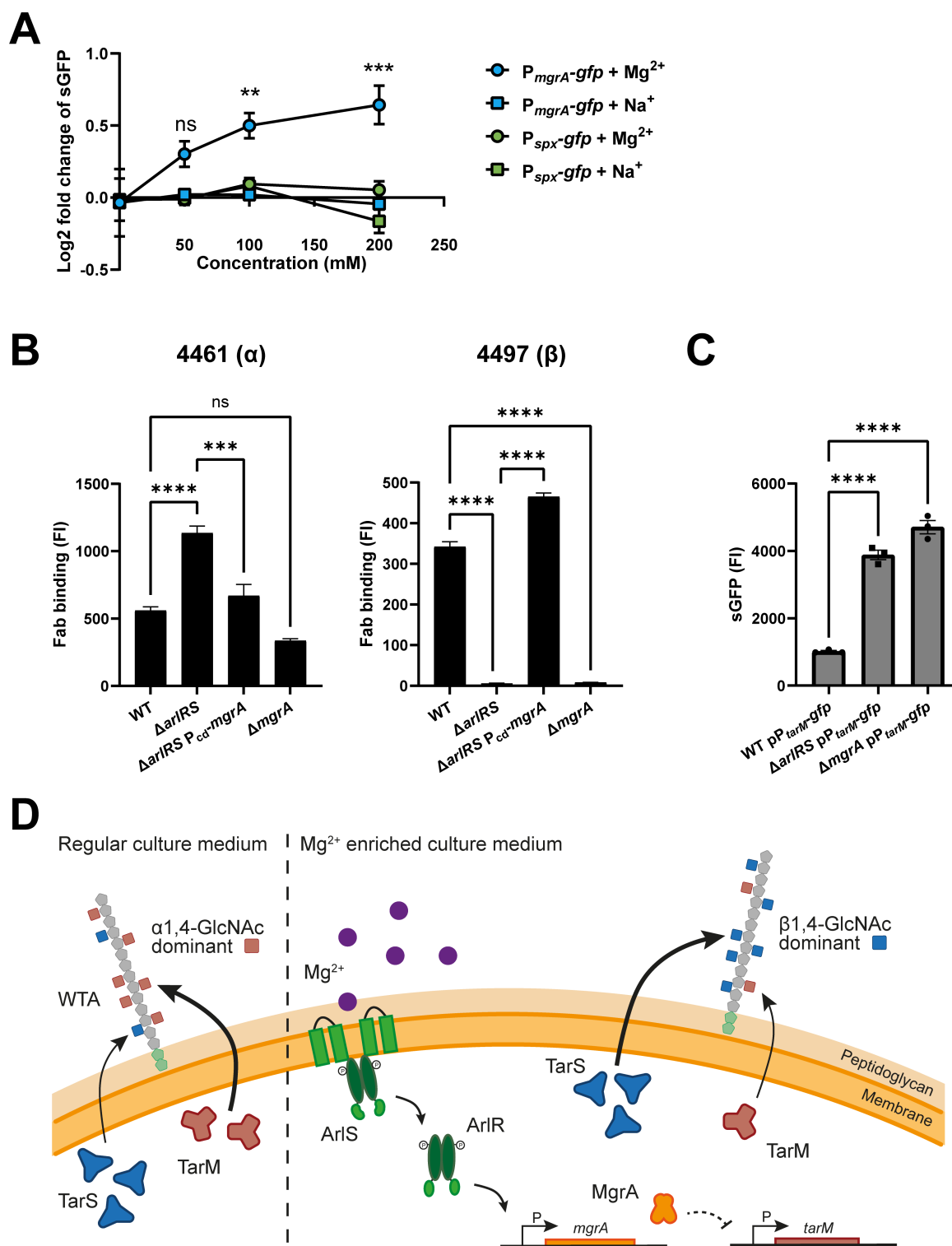


FIG 5 ArlRS represses *tarM* expression through MgrA. (A) Promoter activity of *mgrA* and *spX*, displayed as log2 fold change in fluorescence intensity of sGFP in WT $pP_{mgrA}\text{-gfp}$ or WT $pP_{spX}\text{-gfp}$ bacteria grown in TSB supplemented with Mg^{2+} or Na^+ at various concentrations. (B) Levels of α 1,4- and β 1,4-GlcNAc, quantified by binding of Fab fragments 4461 (α) and 4497 (β) to WT, ΔarlRS , $\Delta\text{arlRS } P_{cd}\text{-mgrA}$ and ΔmgrA of *S. aureus* MW2. Data are represented as fluorescence intensity (FI) as analyzed by flow cytometry. (C) sGFP fluorescence as a measure for promoter activity of *tarM* in WT $pP_{tarM}\text{-gfp}$, $\Delta\text{arlRS } pP_{tarM}\text{-gfp}$, and $\Delta\text{mgrA } pP_{tarM}\text{-gfp}$ bacteria as analyzed by flow cytometry and represented as fluorescence intensity (FI). Data represent three biological replicates \pm SEM. Statistical significance was determined using one- (B, C) and two-way (A) ANOVA with Bonferroni statistical hypothesis testing to correct for multiple comparisons. ** $P < 0.01$, *** $P < 0.001$, (Continued on next page)

Fig 5 (Continued)

**** $P < 0.0001$, ns = not significant. (D) Schematic overview of the proposed pathway for ArlRS-regulated WTA glycoswitching. Mg^{2+} activates ArlRS, inducing expression of *mgrA*. *MgrA* in turn either directly or indirectly represses *tarM* expression, allowing TarS to decorate WTA with predominantly β 1,4-GlcNAc.

DISCUSSION

In this study, we have shown that the TCS ArlRS, through the transcriptional regulator *MgrA*, plays an essential role in regulating the specific GlcNAc decoration of the cell wall glycopolymer WTA, affecting phage infection, langerin binding, and antibiotic resistance. In one-third of *S. aureus* isolates, WTA is not only decorated with β 1,4-GlcNAc through the enzyme TarS but is additionally co-decorated with α 1,4-GlcNAc through the accessory enzyme TarM (12). These TarM/TarS-positive bacteria can thereby regulate WTA glycosylation to switch between α 1,4- or β 1,4-GlcNAc-dominant profiles, attuning them to the environmental conditions. The capacity to dynamically regulate the WTA glycoprofile potentially provides a significant survival advantage to *S. aureus* in specific host niches or for antibiotic susceptibility. Moreover, since WTA is a promising target for various alternative treatment options such as vaccines, antibody-dependent therapies, and phage therapy, it is important to understand how WTA glycoswitching is regulated to align antimicrobial strategies with WTA glycosylation profiles during infection.

By screening 1,920 transposon mutants, we identified 230 mutants with a divergent α 1,4- or β 1,4-GlcNAc WTA glycosylation profile. We identified *tarS* and *tarM* as independent hits in the respective antibody screens confirming the validity of the approach. No other genes in the WTA biosynthesis pathway were identified since these mutants are not included in the NTML. Fifteen of the identified genes had regulatory functions including the three TCS ArlRS, AgrCA, and GraRS. Using a panel of isogenic TCS mutants, we confirmed the role of ArlRS in regulating α 1,4- and β 1,4-GlcNAc WTA glycosylation. A lack of ArlRS resulted in a complete loss of β 1,4-GlcNAc, with concomitantly increased WTA α 1,4-GlcNAc decoration. Moreover, the role of ArlRS in regulating the WTA α 1,4/ β 1,4-GlcNAc ratio was non-redundant since the WTA glycosylation phenotype could be restored by plasmid-based *arlRS* complementation in a Δ XV mutant, which lacks all 15 non-essential TCS. We were unable to confirm the contribution of *graRS* and *agrCA* in the regulation of the WTA glycosylation profile, although both TCS have been implicated in the regulation of *tarM* expression (22, 28). This may be explained by the use of different strain backgrounds since the NTML is constructed in the *S. aureus* USA300 JE2 background. The TCS deletion mutants used in this study were in *S. aureus* USA400 MW2 and the previous report on the role of AgrCA in the regulation of WTA glycosylation used *S. aureus* Newman (22). However, strain-specific effects of *agr*-dependent regulation have been previously documented (23). In addition, glycosylation differences were only observed when stimulating the AgrCA pathway with autoinducing peptides, but not when inactivating this pathway through deletion of *agrA* (22). Therefore, the effect of AgrCA on WTA glycosylation profiles may depend on the activity and regulation of the quorum-sensing system of the particular strain and the experimental conditions.

Using a *tarM*-specific GFP-promoter and mRNA expression analysis, we showed that ArlRS-mediated regulation of the WTA glycosylation profile resulted from increased expression of *tarM*, without any apparent changes in *tarS* expression. Similarly, re-analysis of *S. aureus* transcriptome data generated in 44 *in vitro* and *in vivo* mimicking conditions, demonstrated that *tarM* expression is more dynamically regulated, while *tarS* levels remained constant at a relatively high level in all experimental conditions (24, 37). Since the genes of the *tar* WTA biosynthesis operon, including *tarS*, feature similarly stable expression (24, 37), regulation of the WTA glycoprofile may not be possible through regulation of *tarS* without affecting general WTA turnover. Instead, it could take place through regulation of the accessory *tarM* gene located outside of the *tar* operon. As a result of increased transcription, the increased levels of TarM likely outcompete TarS at a functional level due to its higher enzymatic activity (42, 43). *In vitro* biochemical

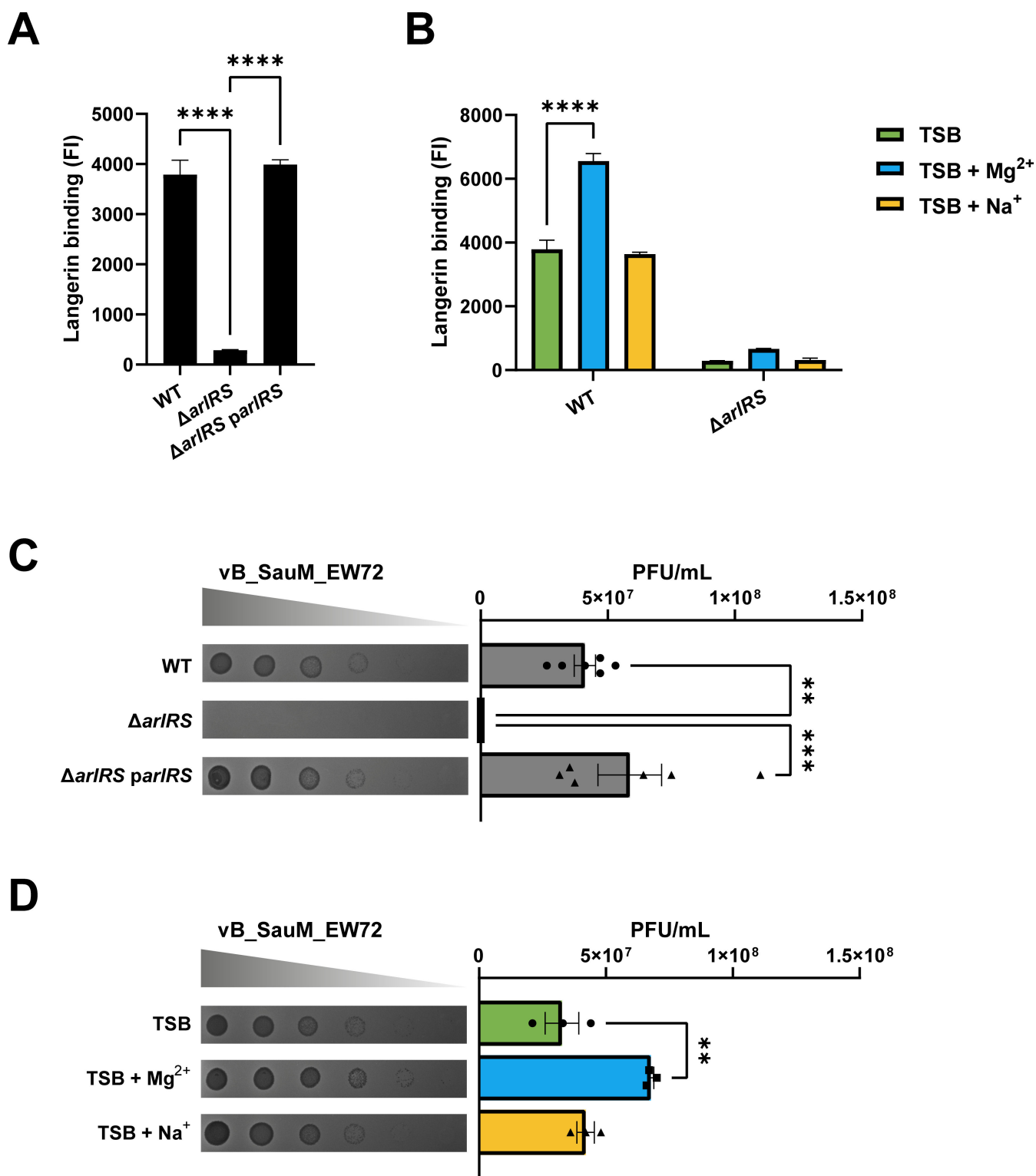


FIG 6 ArlRS activity is required for langerin binding and phage-mediated lysis. (A, B) Binding of recombinant langerin receptor to overnight cultures of (A) WT, $\Delta arlRS$, and $\Delta arlRS parlRS$ bacteria or (B) WT and $\Delta arlRS$ grown in regular TSB or TSB supplemented with 200 mM Mg^{2+} or Na^+ . Data are represented as fluorescence intensity (FI) as analyzed by flow cytometry from three biological replicates. (C, D) Phage dilutions of vB_SauM_EW72 were spotted on a lawn of (C) WT, $\Delta arlRS$ or $\Delta arlRS parlRS$ bacteria or (D) WT bacteria grown in TSB or TSB supplemented with 200 mM Mg^{2+} or Na^+ . Representative images are shown of the formed plaques. PFU/mL was determined from three or six biological replicates. Data are shown as mean \pm SEM. Statistical significance was determined using one- (A, C, D) and two-way (B) ANOVA with Bonferroni statistical hypothesis testing to correct for multiple comparisons. For panels B and D, the mean of each column was compared to the mean of TSB marking only significant comparisons. ** $P < 0.01$, *** $P < 0.001$, **** $P < 0.0001$.

assays with different ratios of recombinant TarM and TarS may be able to confirm this enzymatic competition in the future.

We were able to reduce *tarM* expression and restore WTA β 1,4-GlcNAc glycosylation in the Δ *arlRS* mutant by overexpressing *mgrA*, demonstrating that ArlRS-mediated regulation of *tarM* expression requires *mgrA* and not *spx*. MgrA itself was not identified in our screen since this gene is not included in the NTML. Unexpectedly, the deletion of *mgrA* did not completely phenocopy the *arlRS* mutant. Although the *mgrA* mutant showed a complete loss of β 1,4-GlcNAc similar to the *arlRS* mutant, *mgrA* deletion did not result in a significant concomitant increase in WTA α 1,4-GlcNAc decoration. It is already known that the phenotypes of *arlRS* and the *mgrA* deletion strains show overlap due to overlapping regulons (31, 34, 41, 44), but *tarM* is not part of either regulon (41, 45). A similar observation is made in a recent paper, in which MgrA is identified as the regulator of the *ssc* genes encoding for a novel *S. aureus* secondary glycopolymer, but no canonical *mgrA*-binding site could be found (46). Alternatively, the deletion of *mgrA* may interfere with other regulatory pathways. Indeed, MgrA represses the expression of the transcription factors SarV and AtlR (33), which may indicate that MgrA regulates *tarM* expression indirectly. Therefore, the molecular mechanisms by which MgrA represses *tarM* remain elusive. Furthermore, despite recent advances in RNA sequencing or prediction of transcription factor binding sequences, our observations stress the importance of combining phenotypic screening with experimental work to confirm direct gene regulation (33, 47).

Shifts in WTA glycosylation profiles can be induced by general stress, such as high salt concentrations (21). The medium previously used contained both high Na^+ and Mg^{2+} concentrations. We first demonstrated that salt-induced effects on WTA glycoprofiles were induced by high levels of Mg^{2+} but not Na^+ . We next showed that these Mg^{2+} -induced changes in the WTA glycoprofile depended on the repression of *tarM* promoter activity, which required the ArlRS TCS. Our data extend earlier research on the link between ArlRS, Mg^{2+} , and WTA, where it was shown that ArlRS and Mg^{2+} repressed the *dlt* operon (29), which decorates WTA with D-alanine residues. In addition to transcriptional changes, biochemical studies have shown that Mg^{2+} acts as a co-factor to increase TarS enzymatic activity, which in our conditions may have additionally boosted β 1,4-GlcNAc modifications (43). Unexpectedly, we also detected a slight increase in WTA β 1,4-GlcNAc levels when TSB was supplemented with Na^+ . However, Na^+ did not affect *tarM* or *mgrA* promoter activity. Therefore, these Na^+ -induced effects most likely involved a different pathway independent of ArlRS or MgrA.

Mg^{2+} is an essential mineral for many basic biological processes and one of the four most common cations in the human body (36). Ninety-nine percent of the total amount of Mg^{2+} is found in bones, muscle, and soft tissue (48). The remaining Mg^{2+} is present in red blood cells and serum (48, 49). *S. aureus* can naturally infect the skeletal organ (50). This Mg^{2+} -enriched niche seems to favor chronic infections and induce biofilm formation of *S. aureus* (51, 52). Although in our study Mg^{2+} clearly had a great influence on *S. aureus*, there are no studies yet that analyzed the complete gene set regulated by Mg^{2+} , as has been done for *Streptococcus pyogenes* (53). In *S. pyogenes*, CovS of the streptococcal TCS CovRS has been identified as the sensor for Mg^{2+} and has 32% sequence identity with ArlRS. As no dedicated activation signal for ArlRS has been identified, we propose that Mg^{2+} may be a primary stressor for the ArlRS TCS in *S. aureus*. These findings suggest an important role of metal ion availability in the *S. aureus* WTA glycoswitching. Moreover, it highlights how *S. aureus* could undergo phenotypic WTA modifications in environments with high Mg^{2+} concentrations such as bone, muscle, and soft tissue through the sensing and transcriptional regulation of ArlRS and MgrA.

ArlRS plays a role in several host-pathogen interactions (30–35), including several animal models (31, 33, 34, 44). To probe the potential functional consequences of ArlRS-mediated WTA glycoswitching for biologically relevant interactions, we performed studies to investigate the interaction with human langerin and the impact on infection by β 1,4-GlcNAc-dependent phages. Langerin is a pattern recognition receptor unique

to innate Langerhans cells that specifically binds staphylococcal WTA β -GlcNAc and is hindered by the co-presence of α 1,4-GlcNAc. This interaction acts as the first response in the defense against *S. aureus* in the skin through the induction of skin inflammation specifically neutrophil recruitment (11). As expected, the increased β 1,4-GlcNAc levels in response to high Mg^{2+} and dependence on ArlRS activation resulted in increased Langerin binding. How the conditions in human skin including the concentration of Mg^{2+} would affect ArlRS activation and subsequent WTA glycosylation profiles is currently unknown but warrants further investigation.

With regard to phage infection, the effect of WTA glycoswitching is a double-edged sword. Whereas bacteria may profit from phages to gain favorable genes *via* horizontal gene transfer (4), lytic phages can also kill bacteria (54). WTA decoration with GlcNAc is required for successful infection by siphophages, podophages, and some myophages (5, 15–17), but some phages require GlcNAc to be present in a specific configuration (55). In this study, all used phages depend on the WTA β 1,4-GlcNAc modification to infect and lyse *S. aureus* (22). Consequently, it was expected that phage infection was completely abolished in the $\Delta arlRS$ mutant lacking β 1,4-GlcNAc. This is consistent with a previous observation that after co-culture, *S. aureus* bacteria resistant to the β 1,4-GlcNAc-dependent podophage carried an inactivating mutation in ArlRS (56). In contrast to our finding with langerin and Fab binding experiments, the influence of Mg^{2+} on phage infection was modest. This may be due to the long infection period on the agar plates that did not contain extra Mg^{2+} . Nevertheless, our results still suggest that Mg^{2+} concentrations influence *S. aureus* phage infection. This has relevance for choosing the right phage therapy, as an isolate may be different with regard to WTA glycosylation depending on the location of the infection, such as a osteomyelitis versus endocarditis. Therefore, accurate insight in WTA glycosylation could play a crucial role in preventing future phage therapy failures.

In summary, we identified the critical importance of ArlRS in the dynamic regulation of the WTA GlcNAc decoration in *S. aureus*. ArlRS was activated by high concentrations of Mg^{2+} and subsequently activated MgrA and upregulated *tarM* expression, resulting in WTA glycoswitching from a β 1,4-GlcNAc-dominated to an α 1,4-GlcNAc-dominated profile. As WTA glycosylation patterns impact many biologically relevant and infection-relevant interactions, more research is needed to determine differential GlcNAc levels of *S. aureus* isolates in specific tissues such as bone and skin, common sites of (chronic) *S. aureus* infections. This is especially important since *in vitro* testing of GlcNAc levels in clinical isolates after routine culture or screening for gene presence does not correlate with *in vivo* WTA glycosylation patterns. These explorations could help prioritize the design of new antimicrobial strategies such as vaccines and phage therapy targeting specific WTA glycan modifications.

MATERIALS AND METHODS

Bacterial strains and culture conditions

All *S. aureus* cultures were grown in Tryptic Soy Broth (TSB, Oxoid) overnight at 37°C with continuous shaking. The Nebraska Transposon Mutant Library (NTML; 1,920 arrayed mutants of *S. aureus* strain JE2, harboring both *tarM* and *tarS*) (38) was grown in the presence of 5 μ g/mL erythromycin (Sigma). *S. aureus* complemented strains were grown with the addition of 10 μ g/mL erythromycin or 10 μ g/mL chloramphenicol (Sigma), depending on the resistance marker used. When required, TSB was enriched with $MgCl_2$ (TSB + Mg^{2+} , Merck) or NaCl (TSB + Na^+ , Merck) in a concentration of 200 mM unless stated otherwise. *Escherichia coli* strain DC10B (57) was grown at 37°C with continuous shaking in Lysogeny broth (LB) supplemented with 100 μ g/mL ampicillin (Sigma) when appropriate. All strains used in this study are listed in Table S2.

Analysis of *tarM* and *tarS* mRNA transcription levels

The transcriptome of *S. aureus* HG001 grown in 44 different experimental conditions was analyzed in earlier research (24). The transcript levels of *tarS* (SAOUHSC_00228) and *tarM* (SAOUHSC_00973) were downloaded from the AureoWiki repository (37). Averages of biological replicates were calculated and plotted, comparing *tarM* and *tarS* expressions in all different growth conditions. Statistical difference in the variance of the transcript levels was calculated using an F test with GraphPad Prism 10.2.0.

NTML screen for WTA α 1,4- and β 1,4-*N*-acetylglucosamine glycosylation levels

The protocol for immunoblotting was based on Weber et al. (58) with some modifications. Each of the 1,920 NTML (38) transposon mutants was inoculated from the frozen stock into a single well of a 96-well round bottom plate (Sigma) containing TSB with 5 μ g/mL erythromycin. The next day, 2 μ L of the overnight culture was spotted in duplicate onto Tryptic Soy Agar (TSA, Oxoid) plates containing 5 μ g/mL erythromycin. Cultures of JE2 WT and the markerless deletion mutants of $\Delta tarMS$, $\Delta tarM$, and $\Delta tarS$ in JE2 background were spotted on TSA plates as a control. All plates were incubated overnight and bacteria were transferred from each plate to a 0.45 μ m nitrocellulose membrane (Biorad). Each membrane was dried for 20 min and subsequently washed with demineralized water and Tris-buffered saline (TBS). The membranes were blocked for 1 hour with TBS supplemented with 1% Tween20 (TBST, Fisher Scientific) and 5% bovine serum albumin (BSA; Sigma) and washed with TBST. The glycosylation of each transposon mutant was analyzed using the specific Fab clones 4461 (α 1,4-GlcNAc) and 4497 (β 1,4-GlcNAc) (59) by incubating the membranes for 1 hour with either 0.5 μ g/mL 4461 or 4497 Fabs in TBST. After washing with TBST, the membranes were incubated for 1 hour with a 1:1,000 dilution of Goat Fab Anti-Human IgG Kappa-AP (Southern Biotech) and washed again with TBST. Fab staining, representing WTA glycosylation, was visualized using Vector blue AP Substrate (Vector laboratory). The reaction was stopped with a quick wash with demineralized water and blots were imaged using a Uvitec Platinum V10 imager. Differential glycosylation patterns were assessed by visual comparison of the overall staining intensity of mutants on a single blot.

Bacterial cloning

The deletion mutants $\Delta tarM$, $\Delta tarS$ and the double mutant $\Delta tarMS$ in JE2 background were previously generated (60). MW2 wild-type (WT) bacteria and a panel of cognate TCS deletion mutants were previously generated (25, 44). Complementation mutants of ΔXV and $\Delta arlRS$ were constructed using the pCN51 plasmid under the control of a cadmium promoter, yielding $\Delta XV parlRS$ and $\Delta arlRS parlRS$ (25). Cadmium was not used for the expression of genes as the leaky expression on this plasmid was sufficient to restore the phenotype (25). The *arlRS* deletion mutant complemented with *mgrA* ($\Delta arlRS$ P_{Cd}-*mgrA*) was constructed by Burgui et al. (44) via allelic exchange of the *mgrA* promoter with the cadmium inducible promoter. As this complementation is chromosomal rather than plasmid-based, 5 μ M cadmium was added to the culture medium to reach sufficient *Ar*IRS-independent expression of *mgrA*.

Analysis of α 1,4- and β 1,4-*N*-acetylglucosamine glycosylation levels

WTA glycosylation with either α 1,4- or β 1,4-GlcNAc was analyzed using specific Fab fragments. Overnight cultures in TSB with or without appropriate antibiotics were resuspended in PBS + 0.1% BSA at an optical density 600 nm (OD₆₀₀) of 0.4 and incubated with 3.3 μ g/mL Fab fragments 4461 (α 1,4-GlcNAc) or 4497 (β 1,4-GlcNAc) (59). After washing, bacteria were incubated with 1:200 goat Fab human Kappa IgG Alexa Fluor 647 (Southern Biotech). Bacteria were washed and fixed in 1% paraformaldehyde (PFA, Sigma-Aldrich) and analyzed by flow cytometry (BD FACSCanto II Flow Cytometer, BD Bioscience) using FlowJo version 10 (BD Bioscience).

Promoter activity analysis using *promoter::gfp* translational fusions

Promoter activity of *tarM*, *mgrA*, and *spx* was analyzed using a fluorescent reporter system with the plasmid pCM29, which contains a *SarA*-P1 promoter upstream of sGFP (40). Specific promoter regions of *mgrA*, *spx* (33, 41), and *tarM* (61) were cloned into pCM29 *via* restriction enzyme digest to replace the *SarA*-P1 promoter. Resulting plasmids were first transformed in *E. coli* DC10B and subsequently transformed into MW2 WT (resulting in WT pP_{*mgrA*}-*gfp*, WT pP_{*spx*}-*gfp*, and WT pP_{*tarM*}-*gfp*), in Δ *arlRS* (resulting in Δ *arlRS* pP_{*mgrA*}-*gfp*, Δ *arlRS* pP_{*spx*}-*gfp*, and Δ *arlRS* pP_{*tarM*}-*gfp*) and in Δ *mgrA* (Δ *mgrA* pP_{*tarM*}-*gfp*). Used primers are listed in Table S3.

sGFP-reporter strains were grown overnight in TSB supplemented with 10 μ g/mL chloramphenicol and Mg²⁺ or Na⁺ if appropriate. Cultures were adjusted to an OD₆₀₀ of 0.4 in PBS + 0.1% BSA and fixed with 1% PFA (Sigma-Aldrich). sGFP intensity was analyzed by flow cytometry (BD FACSCanto II Flow Cytometer, BD Bioscience) using FlowJo version 10 (BD Bioscience).

Absolute quantification of mRNA transcripts by reverse transcriptase (RT)-qPCR

As *ArIRS* has an extensive influence on the expression levels of many genes, we quantified the absolute number of mRNA copies for *tarM* and *mgrA* to circumvent the use of reference genes. Briefly, pellets of overnight bacterial cultures were resuspended in TRIzol reagent (Invitrogen) and bacterial cells were disrupted using 0.1 mm zirconium sand and 2 mm glass beads using a Magna-lyser for 2 min at 6,000 rpm. Total RNA was extracted using a Direct-zol RNA miniprep-kit (Zymo Research) according to the manufacturer's protocol followed by a DNase treatment using the Turbo DNA-free kit (Invitrogen). cDNA was synthesized using the Maxima H Minus cDNA Synthesis Master Mix (ThermoFisher) and the absence of genomic DNA was confirmed through no-RT PCRs. RT-qPCR was performed using a standard curve as described by Goerke et al. (62). In short, the genes were amplified with regular PCR using the genomic DNA of *S. aureus* MW2 as a template and primers listed in Table S3. The amplicons were visualized on the gel for specificity, cleaned using GeneJET PCR Purification Kit (Thermo Scientific), and DNA concentration was measured with the Qubit 1X dsDNA HS Assay Kit (Invitrogen) as analyzed with a Qubit 4 Fluorometer. The sequence-specific standard curves of *tarM*, *tarS*, and *mgrA* were then generated using a 10-fold serial dilution (10² to 10⁸ copies/reaction). Quantitative RT-PCR was performed in triplicate on the standard curve and cDNA samples using the PowerTrack SYBR Green Master Mix (Thermo Scientific) in the CFX384 RT-PCR instrument (Bio-Rad) with CFX Maestro 5.0 software. Copy numbers per reaction of samples were determined *via* inter- or extrapolation of the Ct values of cDNA samples.

Langerin binding

S. aureus langerin binding was analyzed as described previously (11, 59). Recombinant FITC-labeled construct of human langerin was kindly provided by Prof. C. Rademacher, University of Vienna, Vienna, Austria (63). In short, overnight cultures were resuspended in TSM buffer (2.4 g/L Tris [Sigma Aldrich], 8.77 g/L, NaCl [Merck], 294 mg/L CaCl₂(H₂O)₂ [Merck], 294 mg/L MgCl₂(H₂O)₆ [Merck], containing 0.1% BSA, pH 7) at an OD₆₀₀ of 0.4 and incubated with 20 μ g/mL recombinant langerin. Langerin binding was analyzed by flow cytometry (BD FACSCanto II Flow Cytometer, BD Bioscience).

Phage spot assay

All phages used in this study are listed in Table S2. Stab20 is a lytic myophage within the genus Kayvirus in the subfamily Twortvirinae (64). The Stab20-like myophages have similar receptor-binding proteins as Stab20 (65). Phage susceptibility of *S. aureus* was tested *via* phage spot assay (22) using the double agar overlay method (66). Briefly, overnight cultures were mixed with phage top agar (20 g/L Nutrient Broth No. 2; 3.5 g/L Agar No. 1 supplemented with 10 mM CaCl₂) and poured over phage base agar (20 g/L

of Nutrient Broth No. 2; 7 g/L Agar No. 1 supplemented with 10 mM CaCl₂) to generate indicator plates. Phage lysates were prepared as described earlier (67) and were diluted to 1 × 10⁸ plaque-forming units (PFU)/mL followed by a 10-fold serial dilution in phage buffer (1 mM MgSO₄, 4 mM CaCl₂, 50 mM Tris-HCl, 100 mM NaCl, pH 8.0). Respective dilutions were spotted on top of the indicator plates. After overnight incubation at 37°C, plaques were counted, PFU/mL determined and plates were imaged (BioRad ChemiDoc XRS + imager).

Statistical analysis

Statistical analysis was performed using GraphPad Prism 10.2.0. The F test was used to compare the variance of two groups, the Student's *t* test and one- and two-way ANOVA with Bonferroni statistical hypothesis testing to correct for multiple comparisons were used to determine significant differences (*P* < 0.05) between two or more groups. All values are reported as mean with standard error of the mean (SEM) of three biological replicates unless indicated otherwise.

ACKNOWLEDGMENTS

We thank S. Man-Bovenkerk for technical assistance, A.R. Temming for providing the Fab clones 4461 and 4497, M. Skurnik for the Stab20 phage, and A. Peschel for the *ΔtarM*, *ΔtarS*, and *ΔtarMS* deletion mutants.

This work was supported by the Vici (09150181910001) research program to N.M.v.S., which is financed by the Dutch Health Council (NWO) and by the Novo Nordisk Foundation, NNF22OC0077593 to E.L. and H.I. and Danmarks Frie Forskningsfond, 2035–00110B to H.I.

AUTHOR AFFILIATIONS

¹Department of Medical Microbiology and Infection Prevention, Amsterdam University Medical Center, University of Amsterdam, Amsterdam, the Netherlands

²Department of Veterinary and Animal Sciences, University of Copenhagen, Copenhagen, Denmark

³Laboratory of Microbial Pathogenesis, Navarrabiomed, Universidad Pública de Navarra, Complejo Hospitalario de Navarra, IdiSNA, Pamplona, Navarra, Spain

⁴Netherlands Reference Laboratory for Bacterial Meningitis, Amsterdam University Medical Center location AMC, Amsterdam, the Netherlands

AUTHOR ORCIDs

Marieke M. Kuijk  <http://orcid.org/0000-0001-8763-2702>
 Emma Tusveld  <http://orcid.org/0009-0003-5244-5730>
 Esther Lehmann  <http://orcid.org/0009-0006-2278-4100>
 Rob van Dalen  <http://orcid.org/0000-0002-0436-6048>
 Iñigo Lasa  <http://orcid.org/0000-0002-6625-9221>
 Hanne Ingmer  <http://orcid.org/0000-0002-8350-5631>
 Yvonne Pannekoek  <https://orcid.org/0000-0003-1154-652X>
 Nina M. van Sorge  <http://orcid.org/0000-0002-2695-5863>

FUNDING

Funder	Grant(s)	Author(s)
Nederlandse Organisatie voor Wetenschappelijk Onderzoek (NWO)	09150181910001	Nina M. van Sorge
Novo Nordisk Fonden (NNF)	NNF22OC0077593	Esther Lehmann Hanne Ingmer

Funder	Grant(s)	Author(s)
Danmarks Frie Forskningsfond (DFF)	2035-00110B	Hanne Ingmer

AUTHOR CONTRIBUTIONS

Marieke M. Kuijk, Data curation, Formal analysis, Investigation, Methodology, Supervision, Writing – original draft, Writing – review and editing | Emma Tusveld, Investigation, Methodology, Validation | Esther Lehmann, Investigation, Methodology, Supervision, Validation, Writing – review and editing | Rob van Dalen, Investigation, Methodology, Supervision, Writing – review and editing | Iñigo Lasa, Investigation, Methodology, Resources, Writing – review and editing | Hanne Ingmer, Methodology, Resources, Supervision, Writing – review and editing | Yvonne Pannekoek, Conceptualization, Methodology, Supervision, Writing – review and editing | Nina M. van Sorge, Conceptualization, Funding acquisition, Investigation, Methodology, Project administration, Resources, Supervision, Writing – original draft, Writing – review and editing

ADDITIONAL FILES

The following material is available [online](#).

Supplemental Material

Fig. S1 (mBio02668-24-s0001.tif). Growth curves.

Fig. S2 (mBio02668-24-s0002.tif). qPCR.

Fig. S3 (mBio02668-24-s0003.tif). Phages.

Fig. S4 (mBio02668-24-s0004.tif). Phages and salts.

Fig. S5 (mBio02668-24-s0005.tif). Antibiotic susceptibility.

Supplemental Material (mBio02668-24-s0006.docx). Supplemental methods, legends for Figures S1-S5 and Table S1, and Tables S2 and S3.

Table S1 (mBio02668-24-s0007.xlsx). NTML mutants showing affected 4461 or 4497 binding levels.

REFERENCES

1. Antimicrobial Resistance Collaborators. 2022. Global burden of bacterial antimicrobial resistance in 2019: a systematic analysis. *Lancet* 399:629–655. [https://doi.org/10.1016/S0140-6736\(21\)02724-0](https://doi.org/10.1016/S0140-6736(21)02724-0)
2. Tacconelli E, Carrara E, Savoldi A, Harbarth S, Mendelson M, Monnet DL, Pulcini C, Kahlmeter G, Kluytmans J, Carmeli Y, Ouellette M, Outtersen K, Patel J, Cavalieri M, Cox EM, Houchens CR, Grayson ML, Hansen P, Singh N, Theuretzbacher U, Magrini N, WHO Pathogens Priority List Working Group. 2018. Discovery, research, and development of new antibiotics: the WHO priority list of antibiotic-resistant bacteria and Tuberculosis. *Lancet Infect Dis* 18:318–327. [https://doi.org/10.1016/S1473-3099\(17\)30753-3](https://doi.org/10.1016/S1473-3099(17)30753-3)
3. Brown S, Xia G, Luhachack LG, Campbell J, Meredith TC, Chen C, Winstel V, Gekeler C, Irazoqui JE, Peschel A, Walker S. 2012. Methicillin resistance in *Staphylococcus aureus* requires glycosylated wall teichoic acids. *Proc Natl Acad Sci U S A* 109:18909–18914. <https://doi.org/10.1073/pnas.1209126109>
4. Winstel V, Liang C, Sanchez-Carballo P, Steglich M, Munar M, Bröker BM, Penadés JR, Nübel U, Holst O, Dandekar T, Peschel A, Xia G. 2013. Wall teichoic acid structure governs horizontal gene transfer between major bacterial pathogens. *Nat Commun* 4:2345. <https://doi.org/10.1038/ncomms3345>
5. Xia G, Corrigan RM, Winstel V, Goerke C, Gründling A, Peschel A. 2011. *Staphylococcus* siphovirus and myovirus wall teichoic acid-dependent adsorption. *J Bacteriol* 193:4006–4009. <https://doi.org/10.1128/JB.01412-10>
6. Winstel V, Kühner P, Salomon F, Larsen J, Skov R, Hoffmann W, Peschel A, Weidenmaier C. 2015. Wall teichoic acid glycosylation governs *Staphylococcus aureus* nasal colonization. *MBio* 6:e00632. <https://doi.org/10.1128/mBio.00632-15>
7. Baur S, Rautenberg M, Faulstich M, Grau T, Severin Y, Unger C, Hoffmann WH, Rudel T, Autenrieth IB, Weidenmaier C. 2014. A nasal epithelial receptor for *Staphylococcus aureus* WTA governs adhesion to epithelial cells and modulates nasal colonization. *PLoS Pathog* 10:e1004089. <https://doi.org/10.1371/journal.ppat.1004089>
8. Lehar SM, Pillow T, Xu M, Staben L, Kajihara KK, Vandlen R, DePalatis L, Raab H, Hazenbos WL, Morisaki JH, et al. 2015. Novel antibody-antibiotic conjugate eliminates intracellular *S. aureus*. *Nature New Biol* 527:323–328. <https://doi.org/10.1038/nature16057>
9. Jung D-J, An J-H, Kurokawa K, Jung Y-C, Kim M-J, Aoyagi Y, Matsushita M, Takahashi S, Lee H-S, Takahashi K, Lee BL. 2012. Specific serum Ig recognizing *Staphylococcus* wall teichoic acid induces complement-mediated opsonophagocytosis against *Staphylococcus aureus*. *J Immunol* 189:4951–4959. <https://doi.org/10.4049/jimmunol.1201294>
10. van Dalen R, Molendijk MM, Ali S, van Kessel KPM, Aerts P, van Strijp JAG, de Haas CJ, Codée J, van Sorge NM. 2019. Do not discard *Staphylococcus aureus* WTA as a vaccine antigen. *Nature New Biol* 572:E1–E2. <https://doi.org/10.1038/s41586-019-1416-8>
11. van Dalen R, De La Cruz Diaz JS, Rumpert M, Fuchsberger FF, van Teijlingen NH, Hanske J, Rademacher C, Geijtenbeek TBH, van Strijp JAG, Weidenmaier C, Peschel A, Kaplan DH, van Sorge NM. 2019. Langerhans cells sense *Staphylococcus aureus* wall teichoic acid through langerin to induce inflammatory responses. *MBio* 10:e00330-19. <https://doi.org/10.1128/mBio.00330-19>
12. Tamminga SM, Völpel SL, Schipper K, Stehle T, Pannekoek Y, van Sorge NM. 2022. Genetic diversity of *Staphylococcus aureus* wall teichoic acid glycosyltransferases affects immune recognition. *Microb Genom* 8:mgen000902. <https://doi.org/10.1099/mgen.0.000902>

13. Xia G, Maier L, Sanchez-Carballo P, Li M, Otto M, Holst O, Peschel A. 2010. Glycosylation of wall teichoic acid in *Staphylococcus aureus* by TarM. *J Biol Chem* 285:13405–13415. <https://doi.org/10.1074/jbc.M109.096172>
14. Winstel V, Xia G, Peschel A. 2014. Pathways and roles of wall teichoic acid glycosylation in *Staphylococcus aureus*. *Int J Med Microbiol* 304:215–221. <https://doi.org/10.1016/j.ijmm.2013.10.009>
15. Li X, Gerlach D, Du X, Larsen J, Stegger M, Kühner P, Peschel A, Xia G, Winstel V. 2015. An accessory wall teichoic acid glycosyltransferase protects *Staphylococcus aureus* from the lytic activity of podoviridae. *Sci Rep* 5:17219. <https://doi.org/10.1038/srep17219>
16. Azam AH, Hoshiga F, Takeuchi I, Miyanaaga K, Tanji Y. 2018. Analysis of phage resistance in *Staphylococcus aureus* SA003 reveals different binding mechanisms for the closely related twort-like phages ϕ SA012 and ϕ SA039. *Appl Microbiol Biotechnol* 102:8963–8977. <https://doi.org/10.1007/s00253-018-9269-x>
17. Estrella LA, Quinones J, Henry M, Hannah RM, Pope RK, Hamilton T, Teneza-Mora N, Hall E, Biswajit B. 2016. Characterization of novel *Staphylococcus aureus* lytic phage and defining their combinatorial virulence using the OmniLog® system. *Bacteriophage* 6:e1219440. <https://doi.org/10.1080/21597081.2016.1219440>
18. Takahashi K, Kurokawa K, Moyo P, Jung DJ, An JH, Chigweshe L, Paul E, Lee BL. 2013. Intradermal immunization with wall teichoic acid (WTA) elicits and augments an anti-*Staphylococcus aureus* IgG response that protects mice from methicillin-resistant *Staphylococcus aureus* infection independent of mannose-binding lectin status. *PLoS One* 8:e69739. <https://doi.org/10.1371/journal.pone.0069739>
19. Howden BP, Giulieri SG, Wong Fok Lung T, Baines SL, Sharkey LK, Lee JYH, Hachani A, Monk IR, Stinear TP. 2023. *Staphylococcus aureus* host interactions and adaptation. *Nat Rev Microbiol* 21:380–395. <https://doi.org/10.1038/s41579-023-00852-y>
20. van Dalen R, Peschel A, van Sorge NM. 2020. Wall teichoic acid in *Staphylococcus aureus* host interaction. *Trends Microbiol* 28:985–998. <https://doi.org/10.1016/j.tim.2020.05.017>
21. Mistretta N, Brossaud M, Telles F, Sanchez V, Talaga P, Rokbi B. 2019. Glycosylation of *Staphylococcus aureus* cell wall teichoic acid is influenced by environmental conditions. *Sci Rep* 9:3212. <https://doi.org/10.1038/s41598-019-39929-1>
22. Yang J, Bowring JZ, Krusche J, Lehmann E, Bejder BS, Silva SF, Bojer MS, Grunert T, Peschel A, Ingmer H. 2023. Cross-species communication via agr controls phage susceptibility in *Staphylococcus aureus*. *Cell Rep* 42:113154. <https://doi.org/10.1016/j.celrep.2023.113154>
23. Jenul C, Horswill AR. 2019. Regulation of *Staphylococcus aureus* virulence. *Microbiol Spectr* 7. <https://doi.org/10.1128/microbiolspec.GPP3-0031-2018>
24. Mäder U, Nicolas P, Depke M, Pané-Farré J, Debarbouille M, van der Kooi-Pol MM, Guérin C, Dérozier S, Hiron A, Jarmer H, Leduc A, Michalik S, Reilman E, Schaffer M, Schmidt F, Bessières P, Noiro P, Hecker M, Msadek T, Völker U, van Dijk JM. 2016. *Staphylococcus aureus* transcriptome architecture: from laboratory to infection-mimicking conditions. *PLoS Genet* 12:e1005962. <https://doi.org/10.1371/journal.pgen.1005962>
25. Villanueva M, García B, Valle J, Rapún B, Ruiz de Los Mozos I, Solano C, Martí M, Penadés JR, Toledo-Arana A, Lasa I. 2018. Sensory deprivation in *Staphylococcus aureus*. *Nat Commun* 9:523. <https://doi.org/10.1038/s41467-018-02949-y>
26. Dubrac S, Boneca IG, Poupel O, Msadek T. 2007. New insights into the Walk/WalR (YycG/YycF) essential signal transduction pathway reveal a major role in controlling cell wall metabolism and biofilm formation in *Staphylococcus aureus*. *J Bacteriol* 189:8257–8269. <https://doi.org/10.1128/JB.00645-07>
27. Bleul L, Francois P, Wolz C. 2021. Two-component systems of *S. aureus*: signaling and sensing mechanisms. *Genes (Basel)* 13:34. <https://doi.org/10.3390/genes13010034>
28. Falord M, Mäder U, Hiron A, Débarbouillé M, Msadek T. 2011. Investigation of the *Staphylococcus aureus* GraSR regulon reveals novel links to virulence, stress response and cell wall signal transduction pathways. *PLoS One* 6:e21323. <https://doi.org/10.1371/journal.pone.0021323>
29. Koprivnjak T, Mlakar V, Swanson L, Fournier B, Peschel A, Weiss JP. 2006. Cation-induced transcriptional regulation of the *dlt* operon of *Staphylococcus aureus*. *J Bacteriol* 188:3622–3630. <https://doi.org/10.1128/JB.188.10.3622-3630.2006>
30. Seidl K, Leemann M, Zinkernagel AS. 2018. The ArlRS two-component system is a regulator of *Staphylococcus aureus*-induced endothelial cell damage. *Eur J Clin Microbiol Infect Dis* 37:289–292. <https://doi.org/10.1007/s10096-017-3130-5>
31. Kwiecinski JM, Crosby HA, Valotteau C, Hippensteel JA, Nayak MK, Chauhan AK, Schmidt EP, Dufrène YF, Horswill AR. 2019. *Staphylococcus aureus* adhesion in endovascular infections is controlled by the ArlRS-MgrA signaling cascade. *PLoS Pathog* 15:e1007800. <https://doi.org/10.1371/journal.ppat.1007800>
32. Walker JN, Crosby HA, Spaulding AR, Salgado-Pabón W, Malone CL, Rosenthal CB, Schlievert PM, Boyd JM, Horswill AR. 2013. The *Staphylococcus aureus* ArlRS two-component system is a novel regulator of agglutination and pathogenesis. *PLoS Pathog* 9:e1003819. <https://doi.org/10.1371/journal.ppat.1003819>
33. Crosby HA, Schlievert PM, Merriman JA, King JM, Salgado-Pabón W, Horswill AR. 2016. The *Staphylococcus aureus* global regulator MgrA modulates clumping and virulence by controlling surface protein expression. *PLoS Pathog* 12:e1005604. <https://doi.org/10.1371/journal.ppat.1005604>
34. Kwiecinski JM, Kratočil RM, Parlet CP, Surewaard BGJ, Kubes P, Horswill AR. 2021. *Staphylococcus aureus* uses the ArlRS and MgrA cascade to regulate immune evasion during skin infection. *Cell Rep* 36:109462. <https://doi.org/10.1016/j.celrep.2021.109462>
35. Radin JN, Kelliher JL, Párraga Solórzano PK, Kehl-Fie TE. 2016. The two-component system ArlRS and alterations in metabolism enable *Staphylococcus aureus* to resist calprotectin-induced manganese starvation. *PLoS Pathog* 12:e1006040. <https://doi.org/10.1371/journal.ppat.1006040>
36. de Baaij JHF, Hoenderop JGJ, Bindels RJM. 2015. Magnesium in man: implications for health and disease. *Physiol Rev* 95:1–46. <https://doi.org/10.1152/physrev.00012.2014>
37. Fuchs S, Mehlan H, Bernhardt J, Hennig A, Michalik S, Surmann K, Pané-Farré J, Giese A, Weiss S, Backert L, Herbig A, Nieselt K, Hecker M, Völker U, Mäder U. 2018. AureoWiki—the repository of the *Staphylococcus aureus* research and annotation community. *Int J Med Microbiol* 308:558–568. <https://doi.org/10.1016/j.ijmm.2017.11.011>
38. Fey PD, Endres JL, Yajjala VK, Widhelm TJ, Boissy RJ, Bose JL, Bayles KW. 2013. A genetic resource for rapid and comprehensive phenotype screening of nonessential *Staphylococcus aureus* genes. *MBio* 4:e00537-12. <https://doi.org/10.1128/mBio.00537-12>
39. Brown EJ, Flygare J, Hazenbos WL, Lehar SM, Mariathasan S, Morisaki JH. 2014. Anti-wall teichoic antibodies and conjugates
40. Pang YY, Schwartz J, Thoendel M, Ackermann LW, Horswill AR, Nauseef WM. 2010. agr-dependent interactions of *Staphylococcus aureus* USA300 with human polymorphonuclear neutrophils. *J Innate Immun* 2:546–559. <https://doi.org/10.1159/000319855>
41. Crosby HA, Tiwari N, Kwiecinski JM, Xu Z, Dykstra A, Jenul C, Fuentes EJ, Horswill AR. 2020. The *Staphylococcus aureus* ArlRS two-component system regulates virulence factor expression through MgrA. *Mol Microbiol* 113:103–122. <https://doi.org/10.1111/mmi.14404>
42. Sobhanifar S, Worrall LJ, Gruninger RJ, Wasney GA, Blaukopf M, Baumann L, Lameignere E, Solomonson M, Brown ED, Withers SG, Strynadka NCJ. 2015. Structure and mechanism of *Staphylococcus aureus* TarM, the wall teichoic acid α -glycosyltransferase. *Proc Natl Acad Sci U S A* 112:E576–85. <https://doi.org/10.1073/pnas.1418084112>
43. Sobhanifar S, Worrall LJ, King DT, Wasney GA, Baumann L, Gale RT, Nosella M, Brown ED, Withers SG, Strynadka NCJ. 2016. Structure and mechanism of *Staphylococcus aureus* TarS, the wall teichoic acid β -glycosyltransferase involved in methicillin resistance. *PLoS Pathog* 12:e1006067. <https://doi.org/10.1371/journal.ppat.1006067>
44. Burgui S, Gil C, Solano C, Lasa I, Valle J. 2018. A systematic evaluation of the two-component systems network reveals that ArlRS is A key regulator of catheter colonization by *Staphylococcus aureus*. *Front Microbiol* 9:342. <https://doi.org/10.3389/fmicb.2018.00342>
45. Luong TT, Dunman PM, Murphy E, Projan SJ, Lee CY. 2006. Transcription profiling of the *Staphylococcus aureus* regulon in *Staphylococcus aureus*. *J Bacteriol* 188:1899–1910. <https://doi.org/10.1128/JB.188.5.1899-1910.2006>

46. Lei MG, Jorgenson MA, Robbs EJ, Black IM, Archer-Hartmann S, Shalygin S, et al. 2024. Characterization of Ssc, an N-acetylgalactosamine-containing *Staphylococcus aureus* surface polysaccharide. *J Bacteriol* 206:e0004824. <https://doi.org/10.1128/jb.00048-24>
47. Manna AC, Ingavale SS, Maloney M, van Wamel W, Cheung AL. 2004. Identification of *Staphylococcus aureus* (SA2062), a new transcriptional regulator, is repressed by SarA and MgrA (SA0641) and involved in the regulation of autolysis in *Staphylococcus aureus*. *J Bacteriol* 186:5267–5280. <https://doi.org/10.1128/JB.186.16.5267-5280.2004>
48. Jahnke-Dechent W, Ketteler M. 2012. Magnesium basics. *Clin Kidney J* 5:i3–i14. <https://doi.org/10.1093/ndtplus/sfr163>
49. Ebel H, Günther T. 1980. Magnesium metabolism: a review. *J Clin Chem Clin Biochem* 18:257–270. <https://doi.org/10.1155/cclm.1980.18.5.257>
50. Urish KL, Cassat JE. 2020. *Staphylococcus aureus* osteomyelitis: bone, bugs, and surgery. *Infect Immun* 88:e00932-19. <https://doi.org/10.1128/IAI.00932-19>
51. Reffuveille F, Josse J, Velard F, Lamret F, Varin-Simon J, Dubus M, Haney EF, Hancock REW, Mongaret C, Gangloff SC. 2018. Bone environment influences irreversible adhesion of a methicillin-susceptible *Staphylococcus aureus* strain. *Front Microbiol* 9:2865. <https://doi.org/10.3389/fmicb.2018.02865>
52. García-Betancur J-C, Goñi-Moreno A, Horger T, Schott M, Sharan M, Eikmeier J, Wohlmuth B, Zernecke A, Ohlsen K, Kuttler C, Lopez D. 2017. Cell differentiation defines acute and chronic infection cell types in *Staphylococcus aureus*. *Elife* 6:e28023. <https://doi.org/10.7554/eLife.28023>
53. Gryllos I, Grifantini R, Colaprico A, Jiang S, Deforce E, Hakansson A, Telford JL, Grandi G, Wessels MR. 2007. Mg(2+) signalling defines the group A streptococcal CsrRS (CovRS) regulon. *Mol Microbiol* 65:671–683. <https://doi.org/10.1111/j.1365-2958.2007.05818.x>
54. Hatoum-Aslan A. 2021. The phages of staphylococci: critical catalysts in health and disease. *Trends Microbiol* 29:1117–1129. <https://doi.org/10.1016/j.tim.2021.04.008>
55. Moller AG, Lindsay JA, Read TD. 2019. Determinants of phage host range in *Staphylococcus* species. *Appl Environ Microbiol* 85:e00209-19. <https://doi.org/10.1128/AEM.00209-19>
56. Głowacka-Rutkowska A, Gozdek A, Empel J, Gawor J, Żuchniewicz K, Kozińska A, Dębski J, Gromadka R, Łobocka M. 2018. The ability of lytic staphylococcal podovirus vB_SauP_phiAGO1.3 to coexist in equilibrium with its host facilitates the selection of host mutants of attenuated virulence but does not preclude the phage antistaphylococcal activity in a nematode infection model. *Front Microbiol* 9:3227. <https://doi.org/10.3389/fmicb.2018.03227>
57. Monk IR, Shah IM, Xu M, Tan MW, Foster TJ. 2012. Transforming the untransformable: application of direct transformation to manipulate genetically *Staphylococcus aureus* and *Staphylococcus epidermidis*. *MBio* 3:e00277-11. <https://doi.org/10.1128/mBio.00277-11>
58. Weber BS, Ly PM, Feldman MF. 2017. Screening for secretion of the type VI secretion system protein hcp by enzyme-linked immunosorbent assay and colony blot. *Methods Mol Biol* 1615:465–472. https://doi.org/10.1007/978-1-4939-7033-9_32
59. Hendriks A, van Dalen R, Ali S, Gerlach D, van der Marel GA, Fuchsberger FF, Aerts PC, de Haas CJC, Peschel A, Rademacher C, van Strijp JAG, Codée JDC, van Sorge NM. 2021. Impact of glycan linkage to *Staphylococcus aureus* wall teichoic acid on langerin recognition and langerhans cell activation. *ACS Infect Dis* 7:624–635. <https://doi.org/10.1021/acscinfecdis.0c00822>
60. Krusche J, Beck C, Lehmann E, Gerlach D, Wolz C, Peschel A. 2024. Systematic classification of phage receptor-binding proteins predicts surface glycopolymer structure in *Staphylococcus* pathogens. *bioRxiv*. <https://doi.org/10.1101/2024.03.04.583386>
61. Prados J, Linder P, Redder P. 2016. TSS-EMOTE, a refined protocol for a more complete and less biased global mapping of transcription start sites in bacterial pathogens. *BMC Genomics* 17:849. <https://doi.org/10.1186/s12864-016-3211-3>
62. Goerke C, Köller J, Wolz C. 2006. Ciprofloxacin and trimethoprim cause phage induction and virulence modulation in *Staphylococcus aureus*. *Antimicrob Agents Chemother* 50:171–177. <https://doi.org/10.1128/AAC.50.1.171-177.2006>
63. Hanske J, Schulze J, Aretz J, McBride R, Loll B, Schmidt H, Knirel Y, Rabsch W, Wahl MC, Paulson JC, Rademacher C. 2017. Bacterial polysaccharide specificity of the pattern recognition receptor langerin is highly species-dependent. *J Biol Chem* 292:862–871. <https://doi.org/10.1074/jbc.M116.751750>
64. Oduor JMO, Kiljunen S, Kadija E, Mureithi MW, Nyachio A, Skurnik M. 2019. Genomic characterization of four novel *Staphylococcus myoviruses*. *Arch Virol* 164:2171–2173. <https://doi.org/10.1007/s00705-019-04267-0>
65. Whittard E, Redfern J, Xia G, Millard A, Ragupathy R, Malic S, Enright MC. 2021. Phenotypic and genotypic characterization of novel polyvalent bacteriophages with potent *Staphylococcus aureus* activity against an international collection of genetically diverse *Staphylococcus aureus*. *Front Cell Infect Microbiol* 11:698909. <https://doi.org/10.3389/fcimb.2021.698909>
66. Kropinski AM, Mazzocco A, Waddell TE, Lingohr E, Johnson RP. 2009. Enumeration of bacteriophages by double agar overlay plaque assay 69–76. In Clokie MRJ, Kropinski AM (ed), *Bacteriophages: methods and protocols*, volume 1: isolation, characterization, and interactions. Humana Press, Totowa, NJ.
67. Bowring JZ, Su Y, Alsaadi A, Svenningsen SL, Parkhill J, Ingmer H. 2022. Screening for highly transduced genes in *Staphylococcus aureus* revealed both lateral and specialized transduction. *Microbiol Spectr* 10:e0242321. <https://doi.org/10.1128/spectrum.02423-21>